

# Plasticized Polymer Composite Single-Ion Conductors for Lithium Batteries

Hui Zhao,<sup>†,||</sup> Fadi Asfour,<sup>‡,||</sup> Yanbao Fu,<sup>†</sup> Zhe Jia,<sup>†</sup> Wen Yuan,<sup>†</sup> Ying Bai,<sup>†,§</sup> Min Ling,<sup>†</sup> Heyi Hu,<sup>‡</sup> Gregory Baker,<sup>‡</sup> and Gao Liu<sup>\*,†</sup>

<sup>†</sup>Energy Storage and Distributed Resources Division, Energy Technologies Area, Lawrence Berkeley National Laboratory, Berkeley, California 94720, United States

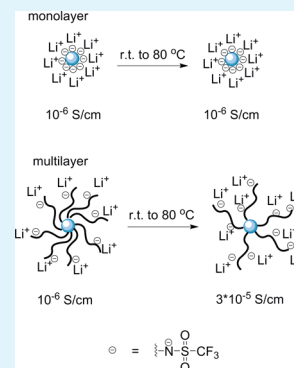
<sup>‡</sup>Department of Chemistry, Michigan State University, East Lansing, Michigan 48824, United States

<sup>§</sup>Beijing Key Laboratory of Environmental Science and Engineering, School of Material Science and Engineering, Beijing Institute of Technology, Beijing 100081, China

## S Supporting Information

**ABSTRACT:** Lithium bis(trifluoromethane) sulfonamide (TFSI) is a promising electrolyte salt in lithium batteries, due to its good conductivity and high dissociation between the lithium cation and its anion. By tethering *N*-pentane trifluoromethane sulfonamide (CSNHTf), a TFSI analogue molecule, onto the surface of silica nanoparticle as a monolayer coverage should increase the Li<sup>+</sup> transference number to unity since anions bound to particles have reduced mobilities. Silica polymer composite has better mechanical property than that of the pure PEO. Analogously trifluoromethane sulfonic aminoethyl methacrylate (TfMA), a TFSI analogue vinyl monomer, was polymerized on silica nanoparticle surface as a multilayer coverage. Anchored polyelectrolytes to particle surfaces offer multiple sites for anions, and in principle the carrier concentration would increase arbitrarily and approach the carrier concentration of the bulk polyelectrolyte. Monolayer grafted nanoparticles have a lithium content of  $1.2 \times 10^{-3}$  g Li/g, and multilayer grafted nanoparticles have a lithium content over an order higher at  $2 \times 10^{-2}$  g Li/g. Electrolytes made from monolayer grafted particles exhibit a weak conductivity dependence on temperature, exhibiting an ionic conductivity in the range of  $10^{-6}$  S/cm when temperatures increase to 80 °C. While electrolytes made from multilayer grafted particles show a steep increase in conductivity with temperature with an ionic conductivity increase to  $3 \times 10^{-5}$  S/cm at 80 °C, with an O/Li ratio of 32.

**KEYWORDS:** lithium battery, polymer-grafted silica nanoparticle, solid-state electrolyte, silica nanoparticle, TFSI, poly(ethylene oxide)



## INTRODUCTION

Lithium ion batteries (LIBs) are the most popular type of rechargeable battery for portable electronics, due to their high energy density and no memory effect.<sup>1–3</sup> The electrolytes used for LIBs are normally composed of highly polar solvents such as carbonate derivatives<sup>4–6</sup> or poly(ethylene oxide) (PEO) and lithium salts such as LiPF<sub>6</sub>, LiBOB, LiCF<sub>3</sub>SO<sub>3</sub>, Li[N(SO<sub>2</sub>CF<sub>3</sub>)<sub>2</sub>] (LiTFSI),<sup>7</sup> Li[N(SO<sub>2</sub>C<sub>2</sub>F<sub>5</sub>)<sub>2</sub>] (LiBETI),<sup>8</sup> and so forth. Lithium bis(trifluoromethane) sulfonamide (LiTFSI) was first brought to the application of lithium ion electrolytes by Armand and Gorecki.<sup>9</sup> LiTFSI is less toxic and more stable than the widely used lithium hexafluorophosphate. There are two trifluoromethane sulfone groups attached to the nitrogen. The electron withdrawing group makes the negative charge delocalized to the large anion structure; this weakens the electrostatic interaction between the anion and cation, enabling a large degree of dissociation. Ue and co-workers studied dissociation the degree of common lithium salts which followed this order: Li[N(SO<sub>2</sub>CF<sub>3</sub>)<sub>2</sub>] > LiAsF<sub>6</sub> > LiPF<sub>6</sub> > LiClO<sub>4</sub> > LiBF<sub>4</sub> > LiC<sub>4</sub>F<sub>9</sub>SO<sub>3</sub> > LiCF<sub>3</sub>SO<sub>3</sub>.<sup>10</sup>

High molecular weight poly(ethylene oxide) (PEO) mixed with lithium salt has been used as solid polymeric electrolyte.<sup>11</sup>

Use of this material could potentially avoid lithium dendrite formation in LIBs and address safety issues. Both anions and cations contribute to the ionic conductivity. Typically, in such polymer electrolytes, lithium cations only contribute to 10–20% of the whole conductivity. With a lithium transference number ( $t_{Li^+}$ ) of 0.1–0.3, the anion mobility is the dominant species in the ionic conductivity of the electrolytes. This low  $t_{Li^+}$  leads to the accumulation of ions close to the surface of one electrode and depletion of ions on the other, resulting in a concentration polarization during the charging and discharging process. Such clustering of ions forms a concentration gradient and limits power density, thereby resulting in an increased internal resistance that generates heat and affects the chemical stability of the electrolyte. For high power LIBs for electric vehicles (EVs), the concentration polarization caused by low lithium transference number of the electrolyte materials could be a serious problem.<sup>12</sup>

Received: July 7, 2015

Accepted: August 18, 2015

Published: August 18, 2015

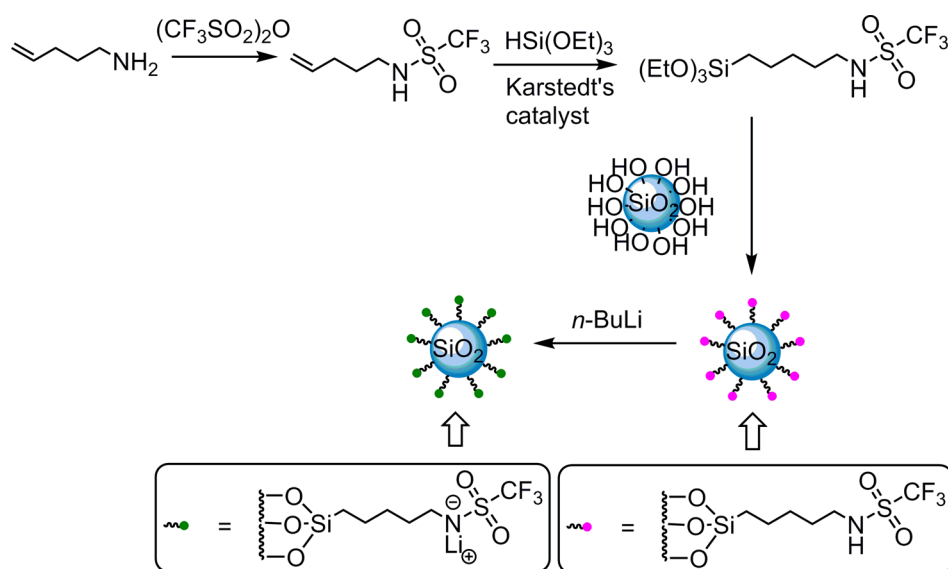


**Figure 1.** Synthetic route for Si-C5NHTf and lithiation to Si-C5NTfLi.

An effective approach to increasing the lithium transference number is to chemically attach the anions on the polymer chains, limiting anion mobility and constructing a single ion conductor.<sup>13–16</sup> A good anion structure should enable the dissociation between the lithium cation and counterion, which could increase the mobile lithium cation concentration in the electrolyte. A salt such as TFSI has an interesting structure that can be used in the construction of single ion conductors. In this study, we tethered two TFSI analogue structures onto silica nanoparticle surfaces and employed polyethylene glycol dimethyl ether with a molecular weight of 500 (PEGDME500) as a solvent for lithium ion transport. Silica particles also increase the mechanical stability and processability of the electrolyte. In this manner, by immobilizing anions on nanoparticles, an increase in the  $\text{Li}^+$  transference number to unity is anticipated.

## RESULTS AND DISCUSSION

**Monolayer-Grafted Nanoparticles.** The synthetic sequence shown in Figure 1 was employed to anchor the salts. A five carbon tether places the salt at a reasonable distance from the surface. 1-Pentylamine was synthesized following a literature procedure.<sup>17</sup> Formation of the trifluoromethylsulfonimide employed triflic anhydride. Hydrosilylation of the resulting alkene with triethoxysilane employed the use of Karstedt's catalyst.

IR spectra of the modified silica demonstrate successful anchoring of the sulfonimide (Figure 2a). The IR spectrum of silica nanoparticle exhibits a sharp peak at  $3750\text{ cm}^{-1}$  corresponding to the free Si–OH stretching. Near-complete loss of the O–H band and the appearance of bands for the imide at  $2800\text{--}3000\text{ cm}^{-1}$  (CH stretching) and at  $1443$  and  $1369\text{ cm}^{-1}$  (sulfonyl asymmetric and symmetric stretching) confirm attachment of the imide. The expected  $\text{CF}_3$  band was obscured by intense bands from the fumed silica. We are unable to observe the N–H stretch of the sulfonimide, as reported by others working on similar systems. Jezorek et al. characterized alkyl amines bound to silica surfaces and found it difficult to observe the amine stretch.<sup>18</sup> Only after the amine was chemically modified did evidence of the amine become apparent. In a similar manner, the existence of the amine is

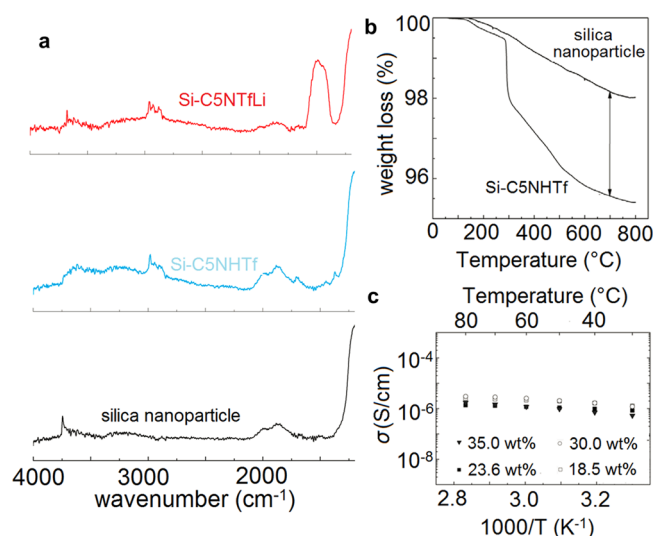


**Figure 2.** (a) FTIR and (b) TGA of the bare silica nanoparticles, Si-C5NHTf, and Si-C5NTfLi. (c) Temperature dependent conductivity for the Si-C5NHTf mixed with PEGDME500.

supported by the appearance of a broad peak at  $1470\text{ cm}^{-1}$  after lithiation, which is attributed to the  $\text{SO}_2$  asymmetric and symmetric stretches of the sulfonimide salt.<sup>19,20</sup>

To explore the deprotonation conditions, a small molecule model, *N*-pentylsulfonimide, was exposed to *n*-butyllithium in toluene. As shown in Supporting Information Figure S2, the NH stretch at  $3250\text{ cm}^{-1}$  is lost upon deprotonation by *n*-butyllithium under these conditions. The ease in forming the sulfonamide salt supports the salt formation of the silica bound sulfonimides.

Figure 2b depicts the thermogravimetric analysis (TGA) data for silica bare nanoparticles versus Si-C5NHTf. The surface coverage of silanol groups on the silica nanoparticle is  $\sim 1.0\text{ mmol/g}$ .<sup>21</sup> Assuming that the alkyl sulfonimide is attached to the silica through each of the alkoxy groups, complete coverage of the nanoparticles with  $0.33\text{ mmol}$  of imide ( $81\text{ mg}$ ) would result in a modified silica with 7.9% of the mass as the bound imide. The extent of surface coverage can be probed by TGA

experiments run in air. Assuming all decomposition products of the imide are volatile, the resulting weight loss should be at most 7.9%. The measured weight loss for the functionalized silica was 2.6%, corresponding to 36% surface coverage, or 0.12 mmol/g silica (Figure 3). If each sulfonimide is converted to

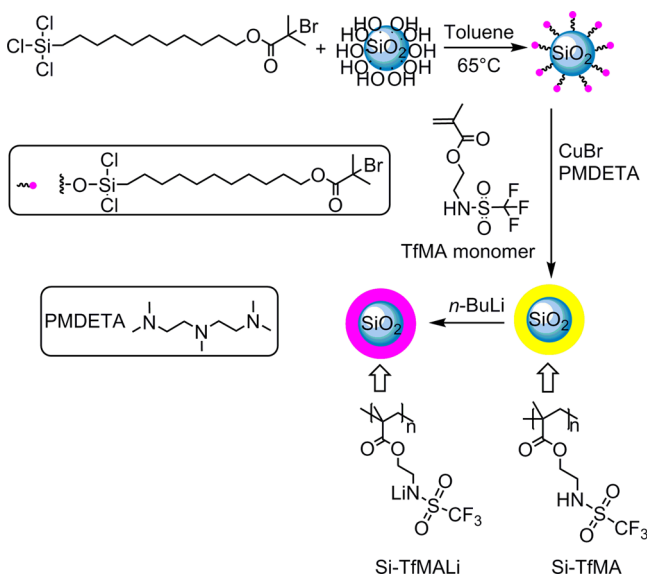


**Figure 3.** Synthetic approach for silica nanoparticles grafted by lithiated poly(trifluoromethane sulfonic aminoethyl methacrylate) (Si-TfMALi).

the corresponding lithium salt upon reaction with butyl lithium, then the maximum lithium carrier concentration in an electrolyte would be  $7.2 \times 10^{-4}$  g Li/g sample.

To experimentally quantify the lithium content in the synthesized Si-CSNTfLi, after TGA under air, lithium content in the TGA residue should be in the form of salts or metal oxides; both are water-soluble and can be analyzed by inductive coupled plasma (ICP) optical emission spectrometry. For the ICP analysis, the TGA residue was stirred in water for 12 h and then filtered prior to the analysis. This combined TGA-ICP characterization results in a lithium content of  $1.2 \times 10^{-3}$  g Li/g sample. This measured value is 1.7 times higher than the calculated lithium content. Presumably because there are three alkoxide groups in each alkyl sulfonimide molecule, we assumed all three alkoxide groups react with the silanol group on silica nanoparticle surface. In reality, as long as one or two alkoxide groups react with silanol, the alkyl sulfonimide molecule is already tethered on the particle surface.

The movement of ions is directly coupled to polymer chain mobility,<sup>22,23</sup> this behavior is thermally activated and is often described by Vogel–Tammann–Fulcher (VTF) equation (eq 1)<sup>24–26</sup>

$$\sigma = \sigma_0 \exp -E_a(T - T_0) \quad (1)$$

where  $\sigma_0$  is the pre-exponential factor related to number of charge carriers,  $E_a$  is the apparent activation energy for ion transport, and  $T_0$  is a parameter related to chain mobility of the polymer. For polymers, a low  $T_g$  should correlate to fast relaxation and high conductivity.

A series of homogeneous electrolytes with various particle contents of Si-CSNTfLi in PEGDME500 were prepared to investigate the conductivity. Electrolytes with low silica loadings (10–25 wt %) are pastes while higher loadings (30–50 wt %)

are powders that become pastes upon shearing. The conductivity data for the samples appear in Figure 2c. The conductivities at 30 °C for the 19, 24, 30, and 35 wt % composites were  $\sim 10^{-6}$  S/cm. The conductivities of the 10, 15, and 50 wt % composites could not be determined due to the low concentration of charge carriers ( $\text{Li}^+$ ) in the case of the first two samples. For samples >45 wt %, the low conductivity stems from poor connectivity, i.e. the volume fraction of PEGDME500 is too low to be continuous throughout the electrolyte.

Lithium concentrations in polyether electrolytes are often expressed as the ratio of ether oxygen to lithium ion. One concern with the measured conductivities is a potential contribution to the conductivity from residual silanols on the surface of the silica particle. These groups also should be lithiated under the conditions used to deprotonate the sulfonimide. To test for conductivity due to the silanols, silica bare particles were treated with *n*-butyllithium using the same protocol for the synthesis of Si-CSNTfLi. A composite of 30 wt % prepared from the lithiated silica and PEGDME500 was analyzed by impedance spectroscopy. The conductivity of the composite was  $< 10^{-8}$  S/cm, the detection limit of the AC impedance analyzer. Thus, we conclude that the contribution from lithiated silanols can be neglected.

The ionic conductivity ( $\sigma$ ) at a specific temperature is often expressed as

$$\sigma = nq\mu \quad (2)$$

where  $n$  is the number of charge carriers per unit volume,  $q$  is charge of the carrier, and  $\mu$  is the mobility of the ions. At a specific temperature, the ionic conductivity of a polymer electrolyte is directly related to the number of charge carriers, the charge of the carrier, and mobility of the carrier, eq 1. Since the mobility of  $\text{Li}^+$  should be constant in a homogeneous medium such as PEGDME500, we attempted to increase the conductivity by increasing the number of carriers. Increasing particle content causes discontinuity of the electrolyte materials without attaining high lithium content, because of this low lithium content the conductivity data could not increase even at high temperatures (Figure 2c). To attain higher conductivities would be attained by increasing the lithium content per silica nanoparticle.

**Multilayer-Grafted Nanoparticles.** One way to do so is to introduce a multilayer grafted silica nanoparticle. Employing surface atom transfer radical polymerization (ATRP) would give a dense surface polymer.<sup>27–29</sup> Figure 3 illustrates the proposed monomer, trifluoromethane sulfonic aminoethyl methacrylate (TfMA), for a surface ATRP on the silica nanoparticles. The sulfoimide tail structure is a mimic of TFSI, the synthetic route of TfMA monomer is shown in Figure S1 in the Supporting Information.

The synthetic route to initiator-decorated nanoparticles is illustrated in Figure 3. Synthesis of the attachable 11-(2-bromo-2-methylpropionyloxy)undecyltrichlorosilane followed the procedure reported by Matyjaszewski et al.<sup>30</sup> One end of the organosilane is chemically bound to the surface of silica particles as a monolayer through the reaction between the Si–Cl and surface silanol groups; the other end of organosilane works as an initiator to trigger the surface ATRP. Lithiation with *n*-butyl lithium in dry toluene then leads to Si-TfMALi.

Figure 4a shows TGA curves of TfMA monomer grafted silica particles from 120 to 900 °C. The samples were dried at 90 °C under vacuum before characterization. Since the data

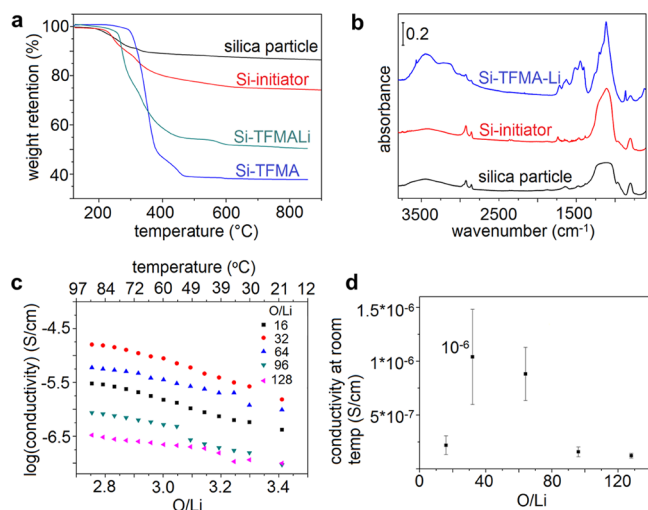


**Figure 4.** (a) TGA and (b) FTIR of the bare silica nanoparticles, Si-initiator, Si-TfMA, and Si-TfMALi. (c) Temperature dependent conductivity and (d) conductivity at 20 °C for the Si-TfMALi mixed with PEGDME500 at various O/Li ratios.

were obtained under air, all organic components of the samples are oxidized to  $\text{CO}_2$  and  $\text{H}_2\text{O}$ , the residue components are silica particles and other nonvolatile inorganic species. Silica particles have a weight loss of 15 wt % at 800 °C, which includes adsorbed water and water formed by condensation of surface bound silanols. After surface polymerization, the large weight loss of sample (62% for Si-TfMA) and (57% for Si-TfMALi) confirmed that a surface polymerization was successfully conducted.

Figure 4b illustrates the FT-IR spectra of the polyTfMA grafted particles at different stages. The IR spectrum of silica particles shows a characteristic broad band centered at  $\sim 790\text{ cm}^{-1}$  associated with Si–O stretch, and a strong and broad absorption band at  $1150\text{ cm}^{-1}$ . After anchoring the ATRP initiator (11-(2-bromo-2-methyl) propionyloxy)-undecyltrichlorosilane to the nanoparticle surface, a new band appeared at  $1730\text{ cm}^{-1}$  (C=O stretch) corresponding to the initiator. Further development of the peak at  $980\text{--}1300\text{ cm}^{-1}$  and split of the peak in the FT-IR spectra corresponds to S=O stretching. The sharp peak at  $680\text{--}780\text{ cm}^{-1}$  was assigned to  $\text{CF}_3$  stretching. Both observations confirm the polymer content at the particle surface.

For electrolytes prepared from binary lithium salts, the conductivity usually increases with decreases in the O/Li ratio, reaching a maximum of  $\sim 20$ . For the monolayer Si-CTNTfLi system, the O/Li ratios reported in Table 1 are an order of magnitude lower than the optimum O/Li ratio of 20. Combined TGA-ICP characterization yields  $2 \times 10^{-2}\text{ g Li/g}$  of multilayer Si-TfMALi sample. Combined with the TGA data, the lithiation efficiency is estimated to be 80%. Table 1 lists the particle weight content of multilayer Si-TfMALi at different O/Li ratios. With this high lithium content ( $2 \times 10^{-2}\text{ g Li/g}$  sample), we are able to obtain O/Li ratios of 32 and 16, similar to that of a bulk polyelectrolyte system, without losing continuity of the PEGDME500 within the composite.

Homogeneous electrolytes with various O/Li ratios ranging from 16 to 128 were prepared by mixing polymer-grafted silica particles and PEGDME500. Figure 4c demonstrates the temperature-dependent ionic conductivity for electrolytes at different O/Li ratios. The conductivities extracted from the

**Table 1. Particle Weight Content for Electrolytes Prepared from Si-CSNTfLi ( $1.2 \times 10^{-3}\text{ g Li/g}$  of Sample) and Si-TfMALi ( $2 \times 10^{-2}\text{ g Li/g}$  of Sample) Dispersed in PEGDME500**

monolayer-grafted nanoparticle (Si-CSNTfLi)	O/Li ratio	185	230	320	425
	particle content (wt %)	35.0	30.0	23.6	18.5
multilayer-grafted nanoparticles (Si-TfMALi)	O/Li ratio	16	32	64	96
	particle content (wt %)	33.2	19.9	11.1	7.7

impedance spectroscopy data are roughly linear, consistent with a thermally activated transport mechanism. Compared to Si-CSNTfLi (Figure 2c), conductivities for the multilayer grafted Si-TfMALi exhibit a steep increase with temperature, over an order of magnitude throughout the temperature range. The room temperature conductivities of Si-TfMALi at different O/Li ratios are compared in Figure 4d, which demonstrates an increase in conductivity with the increase of O/Li ratio. After reaching a peak value of  $10^{-6}\text{ S/cm}$  at an O/Li of 32, the conductivity decreases. As the particle content increases, the PEGDME500 and particle mixture becomes inhomogeneous, resulting in a poor particle dispersion with a corresponding loss of conductivity.

Considering that lithiation efficiency is typically  $\sim 80\%$ , it is therefore a concern that the residual amino groups on the particle surface may be contributing to the measured ionic conductivities. To test this hypothesis, unlithiated Si-TfMA particles were mixed with PEGDME500 and conductivities were measured at different particle contents. The results demonstrate that these composites have conductivities less than  $10^{-8}\text{ S/cm}$ .

**Comparison of the Monolayer and Multilayer Systems.** Figure 5a depicts temperature-dependent conductivities for both monolayer Si-CSNTfLi (O/Li = 425) and multilayer Si-TfMALi (O/Li = 32) samples. Both composite samples have a particle weight fraction of around 19 wt %. The monolayer system suffered from low lithium content, and conductivity remained at the same level with temperature increase. The multilayer system, on the other hand, shows an apparent conductivity increase. Figure 5b illustrates the difference between these two systems.

The monolayer system has ambient temperature conductivity of around  $10^{-6}\text{ S/cm}$ , consistent throughout the studied temperature range. At such low lithium content, any temperature increase does not improve the conductivity. Similarly, polyTfMALi exhibits the same ionic conductivity trend, as it does not have good solubility in PEGDME500; therefore, the multilayer system only has the outer layer of lithium ions accessible to the PEGDME500 solvent at room temperature. Increasing temperature increases the solubility of the polyelectrolyte on particle surface, allowing for the inner part of the multilayer enter into the solution and contribute to conductivity. This results in an order increase in ionic conductivity to around  $3 \times 10^{-5}\text{ S/cm}$ .

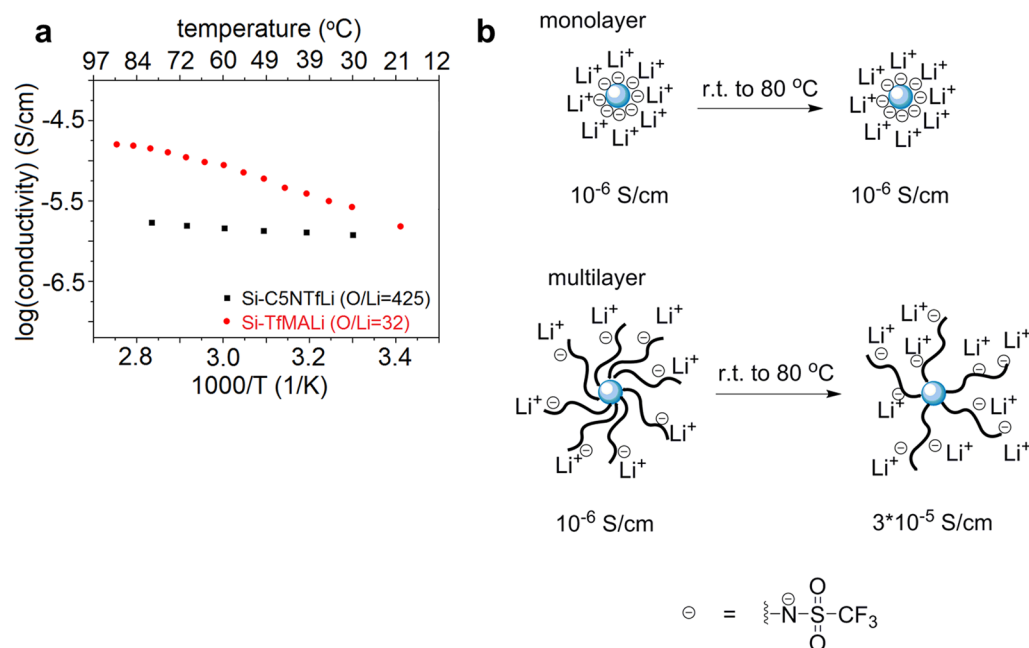


**Figure 5.** (a) Temperature dependent conductivity for Si-C5NTfLi at O/Li 425 and Si-TfMALi at O/Li 32; both samples have particle weight fraction of around 19 wt %. (b) Proposed structural changes of monolayer Si-C5NTfLi (top) and multilayer Si-TfMALi (bottom) from room temperature to 80 °C.

## CONCLUSIONS

Two types of plasticized fume silica-based polymer composite single-ion conductors were successfully developed. Lithium bis(trifluoromethane) sulfonamide (TFSI) analogue structures were grafted onto silica nanoparticles as monolayer and multilayer structures and then mixed with PEGDME500 at varying weight fractions to create composite electrolytes. Optimum room temperature conductivities of both systems was  $10^{-6}$  S/cm; however, electrolytes of monolayer-grafted particles exhibit a weak conductivity dependence. Electrolytes of multilayer grafted particles exhibited a steep increase in ionic conductivity with temperature. It is thought that the increase in temperature increases the solubility of the bound polyelectrolytes, allowing for a greater portion of the multilayer to enter solution and thereby contribute to ionic conductivity, resulting in an order of magnitude increase in conductivity to  $3 \times 10^{-5}$  S/cm at 80 °C. The key to improve ion conducting in a composite system is to improve the ion concentration and polymer chain flexibility next to the particles. The synthetic strategies can be used to improve conductivity in other polymer-based electrolyte systems.

## ASSOCIATED CONTENT

### Supporting Information

The Supporting Information is available free of charge on the ACS Publications website at DOI: 10.1021/acsami.5b06096.

Details about material synthesis and electrochemical data. (PDF)

## AUTHOR INFORMATION

### Corresponding Author

\*Tel: 510-486-7207. Fax: 510-486-7303. E-mail: gliu@lbl.gov.

### Author Contributions

<sup>||</sup>H.Z. and F.A. contributed equally to this work.

## Notes

The authors declare no competing financial interest.

## ACKNOWLEDGMENTS

This work was funded by the Assistant Secretary for Energy Efficiency, Vehicle Technologies Office of the U.S. Department of Energy (U.S. DOE) under the Advanced Battery Materials Research (BMR) and Applied Battery Research (ABR) Programs, supported by the U.S. Department of Energy under Contract # DE-AC02-05 CH11231.

## DEDICATION

Professor Baker passed away in October 2012; this work is dedicated to him.

## ABBREVIATIONS

- CSNHTf, *N*-pentenyl trifluoromethane sulfonamide
- Si-CSNHTf, silica nanoparticle grafted by *N*-pentenyltrifluoromethane sulfonamide
- Si-C5NTfLi, silica nanoparticle grafted by lithiated *N*-pentenyltrifluoromethane sulfonamide
- TfMA, trifluoromethanesulfonic aminoethylmethacrylate
- Si-TfMA, silica nanoparticles grafted by poly-(trifluoromethane sulfonic aminoethyl methacrylate)
- Si-TfMALi, silica nanoparticles grafted by lithiated poly-(trifluoromethanesulfonic aminoethyl methacrylate)
- PEGDME500, polyethylene glycol dimethyl ether with Mw of 500 g/mol

## REFERENCES

- Armand, M.; Tarascon, J. M. Building Better Batteries. *Nature* 2008, 451 (7179), 652–657.
- Zhao, H.; Wang, Z.; Lu, P.; Jiang, M.; Shi, F.; Song, X.; Zheng, Z.; Zhou, X.; Fu, Y.; Abdelbast, G.; Xiao, X.; Liu, Z.; Battaglia, V. S.; Zaghbi, K.; Liu, G. Toward Practical Application of Functional

Conductive Polymer Binder for a High-Energy Lithium-Ion Battery Design. *Nano Lett.* **2014**, *14* (11), 6704–6710.

(3) Zhao, H.; Yuan, W.; Liu, G. Hierarchical Electrode Design of High-Capacity Alloy Nanomaterials for Lithium-Ion Batteries. *Nano Today* **2015**, *10* (2), 193–212.

(4) Shi, F.; Zhao, H.; Liu, G.; Ross, P. N.; Somorjai, G. A.; Komvopoulos, K. Identification of Diethyl 2,5-Dioxahexane Dicarboxylate and Polyethylene Carbonate as Decomposition Products of Ethylene Carbonate Based Electrolytes by Fourier Transform Infrared Spectroscopy. *J. Phys. Chem. C* **2014**, *118* (27), 14732–14738.

(5) Shi, F.; Ross, P. N.; Zhao, H.; Liu, G.; Somorjai, G. A.; Komvopoulos, K. A Catalytic Path for Electrolyte Reduction in Lithium-Ion Cells Revealed by in Situ Attenuated Total Reflection-Fourier Transform Infrared Spectroscopy. *J. Am. Chem. Soc.* **2015**, *137* (9), 3181–3184.

(6) Zhao, H.; Park, S.-J.; Shi, F.; Fu, Y.; Battaglia, V.; Ross, P. N.; Liu, G. Propylene Carbonate (PC)-Based Electrolytes with High Coulombic Efficiency for Lithium-Ion Batteries. *J. Electrochem. Soc.* **2014**, *161* (1), A194–A200.

(7) Alloin, F.; Sanchez, J. Y.; Armand, M. B. Conductivity Measurements of LiTFSI Triblock Copolymers with a Central POE Sequence. *Electrochim. Acta* **1992**, *37* (9), 1729–1731.

(8) Appetecchi, G. B.; Henderson, W.; Villano, P.; Berrettoni, M.; Passerini, S. PEO-LiN (SO 2 CF 2 CF 3) 2 Polymer Electrolytes: I. XRD, DSC, and Ionic Conductivity Characterization. *J. Electrochem. Soc.* **2001**, *148* (10), A1171–A1178.

(9) Armand, M.; Gorecki, W. *Int. Symp. Polym. Electrolytes, 2nd* **1990**, 91.

(10) Ue, M. Mobility and Ionic Association of Lithium and Quaternary Ammonium Salts in Propylene Carbonate and  $\gamma$ -Butyrolactone. *J. Electrochem. Soc.* **1994**, *141* (12), 3336–3342.

(11) Armand, M. B.; Chabagno, J. M.; Duclot, M. In *Second International Meeting on Solid Electrolytes*, University of St Andrews, Fife, Scotland, 1978.

(12) Doyle, M.; Fuller, T. F.; Newman, J. The Importance of the Lithium Ion Transference Number in Lithium/Polymer Cells. *Electrochim. Acta* **1994**, *39* (13), 2073–2081.

(13) Fujinami, T.; Tokimune, A.; Mehta, M. A.; Shriver, D. F.; Rawsky, G. C. Siloxaluminates Polymers with High Li<sup>+</sup> Ion Conductivity. *Chem. Mater.* **1997**, *9* (10), 2236–2239.

(14) Snyder, J. F.; Hutchison, J. C.; Ratner, M. A.; Shriver, D. F. Synthesis of Comb Polysiloxane Polyelectrolytes Containing Oligoether and Perfluoroether Side Chains. *Chem. Mater.* **2003**, *15* (22), 4223–4230.

(15) Sun, X.-G.; Reeder, C. L.; Kerr, J. B. Synthesis and Characterization of Network Type Single Ion Conductors. *Macromolecules* **2004**, *37* (6), 2219–2227.

(16) Sun, X.-G.; Kerr, J. B. Synthesis and Characterization of Network Single Ion Conductors Based on Comb-Branched Polyepoxide Ethers and Lithium Bis(allylmalonato)borate. *Macromolecules* **2006**, *39* (1), 362–372.

(17) Gagne, M. R.; Stern, C. L.; Marks, T. J. Organolanthanide-Catalyzed Hydroamination. A Kinetic, Mechanistic, and Diastereoselectivity Study of the Cyclization of N-unprotected Amino Olefins. *J. Am. Chem. Soc.* **1992**, *114* (1), 275–294.

(18) Fulcher, C.; Crowell, M. A.; Bayliss, R.; Holland, K. B.; Jezorek, J. R. Synthetic Aspects of the Characterization of Some Silica-Bound Complexing Agents. *Anal. Chim. Acta* **1981**, *129* (0), 29–47.

(19) Glemser, O.; Roesky, H. W.; Heinze, P. R. Synthesis of Sulfur Difluoride (Difluorophosphinyl)-imide and Sulfur Oxide Difluoride (Fluorosulfonyl)imide. *Angew. Chem., Int. Ed. Engl.* **1967**, *6* (8), 710–711.

(20) Roesky, H. W. Preparation of Sulfur Oxide (Fluorosulfonyl)-imide and Sulfur Dichloride (Fluorosulfonyl)imide. *Angew. Chem., Int. Ed. Engl.* **1967**, *6* (8), 711–711.

(21) Leonardelli, S.; Facchini, L.; Fretigny, C.; Tougne, P.; Legrand, A. P. Silicon-29 NMR Study of Silica. *J. Am. Chem. Soc.* **1992**, *114* (16), 6412–6418.

(22) Hu, H.; Yuan, W.; Lu, L.; Zhao, H.; Jia, Z.; Baker, G. L. Low Glass Transition Temperature Polymer Electrolyte Prepared from Ionic Liquid Grafted Polyethylene Oxide. *J. Polym. Sci., Part A: Polym. Chem.* **2014**, *52* (15), 2104–2110.

(23) Hu, H.; Yuan, W.; Zhao, H.; Baker, G. L. A Novel Polymer Gel Electrolyte: Direct Polymerization of Ionic Liquid from Surface of Silica Nanoparticles. *J. Polym. Sci., Part A: Polym. Chem.* **2014**, *52* (1), 121–127.

(24) Vogel, H. The Temperature Dependence of the Viscosity of Liquids. *Phys. Z.* **1921**, *22*, 645–646.

(25) Tamman, G.; Hesse, W. Z. The Dependence of Viscosity on Temperature of Supercooled Liquids. *Anorg. Allg. Chem.* **1926**, *156*, 245–257.

(26) Fulcher, G. S. Analysis of Recent Measurement of the Viscosity of Glasses. *J. Am. Ceram. Soc.* **1925**, *8* (6), 339–355.

(27) Yuan, W.; Zhao, H.; Hu, H.; Wang, S.; Baker, G. L. Synthesis and Characterization of the Hole-Conducting Silica/Polymer Nanocomposites and Application in Solid-State Dye-Sensitized Solar Cell. *ACS Appl. Mater. Interfaces* **2013**, *5* (10), 4155–4161.

(28) Jia, Z.; Yuan, W.; Zhao, H.; hu, h.; Baker, G. L. Composite Electrolytes Comprised of Poly(Ethylene Oxide) and Silica Nanoparticles with Grafted Poly(Ethylene Oxide)-Containing Polymers. *RSC Adv.* **2014**, *4*, 41087.

(29) Jia, Z.; Yuan, W.; Sheng, C.; Zhao, H.; Hu, H.; Baker, G. L. Optimizing the Electrochemical Performance of Imidazolium-Based Polymeric Ionic Liquids by Varying Tethering Groups. *J. Polym. Sci., Part A: Polym. Chem.* **2015**, *53* (11), 1339–1350.

(30) Matyjaszewski, K.; Miller, P. J.; Shukla, N.; Immaraporn, B.; Gelman, A.; Luokala, B. B.; Siclovan, T. M.; Kicelbick, G.; Vallant, T.; Hoffmann, H.; Pakula, T. Polymers at Interfaces: Using Atom Transfer Radical Polymerization in the Controlled Growth of Homopolymers and Block Copolymers from Silicon Surfaces in the Absence of Untethered Sacrificial Initiator. *Macromolecules* **1999**, *32* (26), 8716–8724.